

# High-temperature characteristics of $\text{Al}_x\text{Ga}_{1-x}\text{N}/\text{GaN}$ Schottky diodes

Zhang Xiaoling(张小玲)<sup>1,†</sup>, Li Fei(李菲)<sup>1</sup>, Lü Changzhi(吕长志)<sup>1</sup>, Xie Xuesong(谢雪松)<sup>1</sup>,  
Li Ying(李英)<sup>2</sup>, and Mohammad S N<sup>3</sup>

(1 Department of Electronic Information and Control Engineering, Beijing University of Technology, Beijing 100124, China)

(2 Department of Mechanical and Electrical Engineering, Shougang Institute of Technology, Beijing 100041, China)

(3 Department of Electrical & Computer Engineering, Howard University, Washington, DC 20059, USA)

**Abstract:** High-temperature characteristics of the metal/ $\text{Al}_x\text{Ga}_{1-x}\text{N}/\text{GaN}$  M/S/S (M/S/S) diodes have been studied with current–voltage ( $I$ – $V$ ) and capacitance–voltage ( $C$ – $V$ ) measurements at high temperatures. Due to the presence of the piezoelectric polarization field and a quantum well at the  $\text{Al}_x\text{Ga}_{1-x}\text{N}/\text{GaN}$  interface, the  $\text{Al}_x\text{Ga}_{1-x}\text{N}/\text{GaN}$  diodes show properties distinctly different from those of the  $\text{Al}_x\text{Ga}_{1-x}\text{N}$  diodes. For the  $\text{Al}_x\text{Ga}_{1-x}\text{N}/\text{GaN}$  diodes, an increase in temperature accompanies an increase in barrier height and a decrease in ideality factor, while the  $\text{Al}_x\text{Ga}_{1-x}\text{N}$  diodes are opposite. Furthermore, at room temperature, both reverse leakage current and reverse breakdown voltage are superior for the  $\text{Al}_x\text{Ga}_{1-x}\text{N}/\text{GaN}$  diodes to those for the  $\text{Al}_x\text{Ga}_{1-x}\text{N}$  diodes.

**Key words:** Schottky diodes; AlGaN/ GaN; high-temperature

**DOI:** 10.1088/1674-4926/30/3/034001

**PACC:** 7280E; 7360L

## 1. Introduction

Metal/semiconductor/semiconductor (M/S/S) diodes, which produce both Schottky and Ohmic contacts, are of considerable scientific and technological interests. They have many fascinating properties and applicability to electronic, optoelectronic, and electrochemical devices. Many different investigations have been conducted over the years to explore the fundamental basis of their applications as Ohmic and Schottky contacts, but without much success. Yet, with the requirement for ever decreasing size of devices within an integrated circuit, greater understanding of their fundamental basis is called for.

Among various semiconductors, III–V nitrides are currently under extensive investigations for applications to solar-blind photodetectors, lasers, and high-power, high-frequency, high-temperature high electron-mobility transistors (HEMTs)<sup>[1]</sup>. HEMTs suffer from excess gate leakage at high temperatures, and this impedes their gate-control and power consumption capability. The high-temperature noise performance is also affected by the gate leakage current<sup>[2]</sup>. So, these devices must be optimized for low-leakage and high temperature operations.

During the past several years, much effort has been devoted to the study of the III–V nitride M/S heterostructures<sup>[3–9]</sup>. Our objective in this investigation is to extend the scope of those efforts to shed light on the fundamental chemistry, physics, and materials science of M/S/S contacts formed by metal deposition on AlGaN/GaN heterostructures. We are particularly interested in the high-temperature studies of AlGaN/GaN diodes.

## 2. Experimental method

Semiconductor layers were grown on 400  $\mu\text{m}$  thick (0001) sapphire substrate by metal-organic chemical vapor de-

position (MOCVD) method. For the AlGaN/GaN diodes, 60 nm thick GaN buffer layer was first grown on sapphire substrate. It was followed successively by the growth of a 2  $\mu\text{m}$  thick low temperature (500 °C) undoped GaN layer, a 5 nm thick undoped  $\text{Al}_x\text{Ga}_{1-x}\text{N}$  layer, a 10 nm thick ( $5.0 \times 10^{18} \text{ cm}^{-3}$ ) Si-doped  $\text{Al}_x\text{Ga}_{1-x}\text{N}$  layer, and finally a 5 nm thick ( $1.0 \times 10^{19} \text{ cm}^{-3}$ ) Si-doped GaN layer. For the  $\text{Al}_x\text{Ga}_{1-x}\text{N}$  layers, the growth temperature was 1070 °C, and the Al mole fraction was  $x \approx 0.2$ . For comparison, simple  $\text{Al}_x\text{Ga}_{1-x}\text{N}$  M/S Schottky diodes were also grown. For these diodes, 60 nm thick GaN buffer layer was first grown on 400  $\mu\text{m}$  thick sapphire substrate. It was followed successively by the growth of a 1  $\mu\text{m}$  thick lowly doped ( $\sim 3.0 \times 10^{17} \text{ cm}^{-3}$ )  $\text{Al}_x\text{Ga}_{1-x}\text{N}$  layer, and a 5 nm thick ( $5.0 \times 10^{18} \text{ cm}^{-3}$ ) Si-doped GaN layer.

Several samples were cut from each wafer, and they were cleaned first by degreasing in a soap solution, and next by 3 min ultrasonic baths ( $T = 27^\circ\text{C}$ ) successively in trichloroethylene, acetone, and methanol. The samples were then dipped in a heated bath ( $T = 70^\circ\text{C}$ ) of  $\text{NH}_4\text{OH} : \text{H}_2\text{O}_2 : \text{H}_2\text{O}$  (1 : 1 : 5) mixture for 3 min, followed by a 3 min dip in a heated  $\text{HCl} : \text{H}_2\text{O}_2 : \text{H}_2\text{O}$  (1 : 1 : 5) mixture ( $T = 70^\circ\text{C}$ ). To clean the surface further and to make it smoother, the samples were next immersed in boiling aqua regia solution for 5 min. Unfortunately, the  $\text{NH}_4\text{OH} : \text{H}_2\text{O}_2 : \text{H}_2\text{O}$  (1 : 1 : 5) mixture does not remove the surface oxide/hydroxide layers completely from throughout the surface. To overcome this problem, to clean the surface further, and to make it smoother, the samples were next immersed in boiling aqua regia solution for 5 min. The boiling points of  $\text{H}_2\text{O}$ ,  $\text{HCl}$ , and  $\text{HNO}_3$  are 100, 110, and 121.8 °C, respectively. So, the boiling point of the diluted aqua regia solution depended on the concentration of various constituent chemical components. Disappointingly, pure aqua regia solution ( $\text{HNO}_3 : \text{HCl} = 1 : 3$ ) does produce some damage to the surface, which was minimized by optimi-

† Corresponding author. Email: zhangxiaoling@bjut.edu.cn

Received 4 May 2008, revised manuscript received 4 November 2008

© 2009 Chinese Institute of Electronics

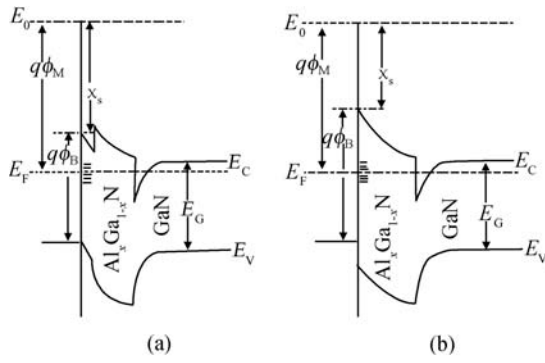


Fig. 1. Schematic diagram of the band structure of (a) Au/Ni/GaN/Al<sub>x</sub>Ga<sub>1-x</sub>N/GaN and (b) metal/Al<sub>x</sub>Ga<sub>1-x</sub>N/GaN Schottky contacts under forward bias.

zing the dilution of the solution. Drouin *et al.*<sup>[10]</sup> noted that by diluting solution of aqua regia to an optimum level (e.g., H<sub>2</sub>O : HNO<sub>3</sub> : HCl = 8 : 1 : 7), it is possible to achieve desired surface treatment, and hence the best possible surface morphology. Following the optimized aqua regia (H<sub>2</sub>O : HNO<sub>3</sub> : HCl = 1 : 2 : 6) treatment, the samples were washed with deionized water. They were kept immersed in methanol during the idle time of processing. The surface is generally very prone to subsequent oxide/hydroxide formation, which adversely affects the contact performance. So efforts were made to prevent the samples from being exposed to air for an extended period of time after they were treated by aqua regia.

Schottky diodes were fabricated using two-step photolithography<sup>[3]</sup>. The Ohmic electrode was the Ti/Al/Pd/Au (200 Å/600 Å/400 Å/500 Å) multilayer contact starting with Ti, and the Schottky electrode was the bilayer Ni/Au (300 Å/1000 Å) contact. Following photolithography, but during evaporation, the base pressure of the vacuum chamber was maintained at about 10<sup>-7</sup> Torr. This procedure was essential to ensure that, during metal deposition, the metal atoms transported toward the semiconductor have only low thermal energy, and that they do not impinge the semiconductor surface hard enough to cause metal induced surface damage, which we called dangling chemical bonds (DCBs). High temperature characterizations of all the diodes are studied by current–voltage (*I*–*V*) and capacitance–voltage (*C*–*V*) measurements. From the *I*–*V* plots reverse/forward voltage drop, reverse saturation current, and breakdown voltage were determined.

A schematic diagram of the band structure of the Al<sub>x</sub>Ga<sub>1-x</sub>N/GaN M/S/S Schottky diode under forward bias is shown in Fig. 1. In this figure, *E<sub>F</sub>* is the Fermi level of the semiconductor band, and *E<sub>0</sub>* is the absolute vacuum level. This Fermi level is positive when above the bottom of the conduction band edge *E<sub>C</sub>*. The GaN layer on the top is only 5 nm thick. The Al<sub>x</sub>Ga<sub>1-x</sub>N layer underneath it has a thickness of one micron. As the GaN/Al<sub>x</sub>Ga<sub>1-x</sub>N layer is an abrupt S/S heterostructure, depending on temperature, there may be diffusion of Al from Al<sub>x</sub>Ga<sub>1-x</sub>N into GaN. With this diffusion, the top GaN, at certain temperature(s), may altogether be converted into Al<sub>x</sub>Ga<sub>1-x</sub>N. So, while Figure 1(a) corresponds to the Au/Ni/GaN/Al<sub>x</sub>Ga<sub>1-x</sub>N/GaN band structure, Figure 1(b) corresponds to the Au/Ni/Al<sub>x</sub>Ga<sub>1-x</sub>N/GaN band structure.

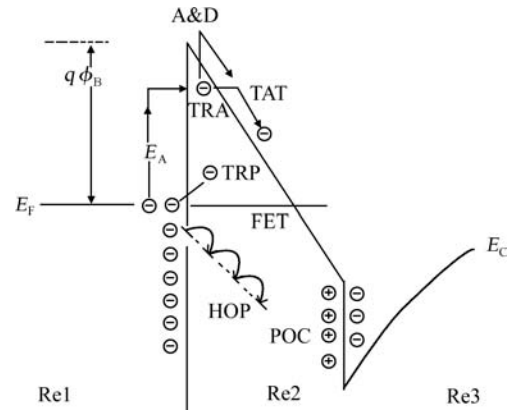


Fig. 2. Schematic diagram showing two-step trap-assisted tunneling, field-emission tunneling, trapping, hopping, in the interface regions of Al<sub>x</sub>Ga<sub>1-x</sub>N/GaN Schottky diodes. In the figure, activation energy is denoted by *E<sub>A</sub>*, deep level trapping by TRP, shallow-level trapping by TRA, two-step trap-assisted tunneling by TAT, activation and drift by A&D, field-emission tunneling by FET, hopping by HOP, polarization charge by POC, metal region 1 by Re1, Al<sub>x</sub>Ga<sub>1-x</sub>N region 2 by Re2, and GaN region 3 by Re3.

### 3. Results and discussions

#### 3.1. Capacitance–voltage characteristics

The *C*–*V* studies explain the characteristics of the depletion region of the M/S/S Schottky diodes. The inverse square of the capacitance, as a function of applied reverse bias, for a diode is given by<sup>[4]</sup>

$$C^{-2} = a_T - b_T V, \quad (1)$$

where *a<sub>T</sub>* and *b<sub>T</sub>* are the constants defined by

$$a_T = \frac{2(qV_{bi} - k_B T)}{q^2 \epsilon_0 \epsilon_s N_d}, \quad (2)$$

$$b_T = \frac{2}{q \epsilon_0 \epsilon_s N_d}, \quad (3)$$

*k<sub>B</sub>* is the Boltzmann constant, *T* is the absolute temperature, *ε<sub>0</sub>* is the permittivity in vacuum, *ε<sub>s</sub>* is the dielectric constant, and *N<sub>d</sub>* is the doping concentration of the Al<sub>x</sub>Ga<sub>1-x</sub>N sample. The built-in potential *V<sub>bi</sub>* is given by

$$V_{bi} = \phi_B - V_n \quad (4)$$

With

$$V_n = \frac{k_B T}{q} \ln \frac{N_c}{N_d}. \quad (5)$$

*N<sub>c</sub>* is the effective density of states for electrons in the conduction band.

At high negative biases, there occurs an upward band bending of the semiconductor. The barrier height at the M/S interface is consequently enlarged, and the probability of the thermionic emission reduced. At high temperatures, metal electrons are thermally activated and transported via a two-step trap-assisted tunneling process (see Fig. 2). These metal electrons are first thermally activated to a trap state at the M/S interface, and then tunnel into the semiconductor. If *E<sub>A</sub>* is the

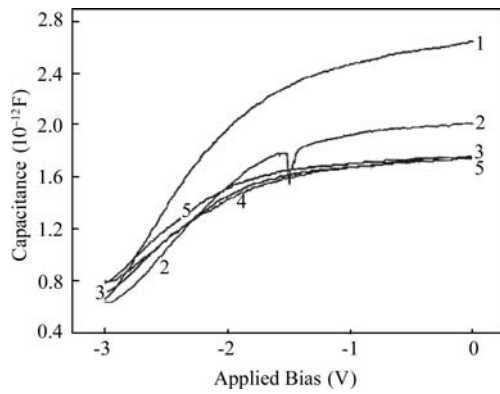


Fig. 3. Variation of capacitance  $C$  with applied bias at various temperatures. Curves 1, 2, 3, 4 and 5 correspond respectively to  $T = 300$ , 200, 150, 100, and 27 °C.

activation energy, then assuming thermal activation as the rate-limiting step, the energy of the trap state is  $\phi_B - E_A$  below the conduction band edge  $E_C$  of the semiconductor. Also, the functional dependence of thermal activation is  $\exp(-E_A/k_B T)$ . Taking the uncertainties in  $E_A$  and  $\phi_B$  into account, the energy level of the trap state may reasonably be assumed to be  $\pm 0.1$  to 0.05 eV. While in the semiconductor depletion region, the electrons can either be captured by ionized donor atoms or be drifted into the quantum well at the  $\text{Al}_x\text{Ga}_{1-x}\text{N}/\text{GaN}$  interface. However, the 2DEG sheet charge density reduces at higher temperature, and there is still some polarization electric field in the strained  $\text{Al}_x\text{Ga}_{1-x}\text{N}/\text{GaN}$  structure. The probability for electrons to be transported and accumulated into the quantum well under the influence of this field is very high. On their way to the quantum well, some of them may be nullified by the polarized induced positive charges. The electrons (e.g., donor atom electrons and host atom electrons) of the  $\text{Al}_x\text{Ga}_{1-x}\text{N}$  layer also acquire higher energy at higher temperatures, and thus, if freed, tend to enter the quantum well leaving behind additional ionized donor atoms. As a result, the depletion layer charges become higher with the depletion layer extending deeper into the semiconductor. The capacitance is consequently increased, which is evident from Fig. 3, which shows the measured temperature dependence of the  $C$ - $V$  characteristics of the  $\text{Al}_x\text{Ga}_{1-x}\text{N}/\text{GaN}$  Schottky contacts. As evident from the figure, the values of the capacitance is different at different temperatures, because, under an applied AC signal, the capacitance depends on the degree of variation of charge transfer to the quantum well. When  $T < 100$  °C, metal electrons are not energetic enough to be activated for transport into the quantum well. Consequently the 2DEG charge is quite insensitive, and there is hardly any change in capacitance as a function of temperature.

The temperature dependence of  $C^{-2}$  versus  $V$  plots is shown in Fig. 4. In this instance,  $C^{-2}$  decreases with increasing temperature because deeper level traps are exposed more by an increase in the depletion region width, and the electrons trapped are emitted in higher numbers at higher temperatures. The concentration and depth of the traps exposed by increasing the depletion region width  $W$  do not vary linearly. The linearity of the  $C^{-2}$  versus  $V$  curves is consequently compromised.

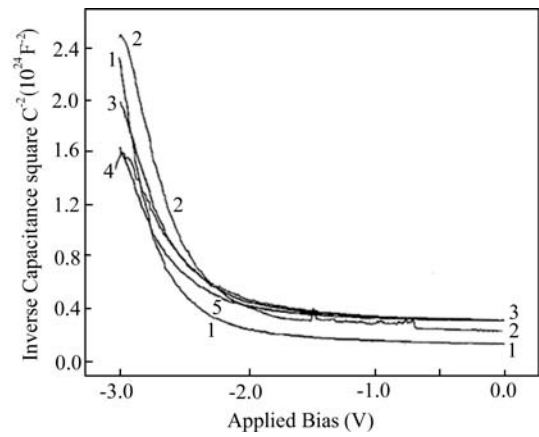


Fig. 4. Variation of inverse-square capacitance  $C^{-2}$  with applied bias at various temperatures. Curves 1, 2, 3, 4, and 5 correspond respectively to 300, 200, 150, 100 and 27 °C.

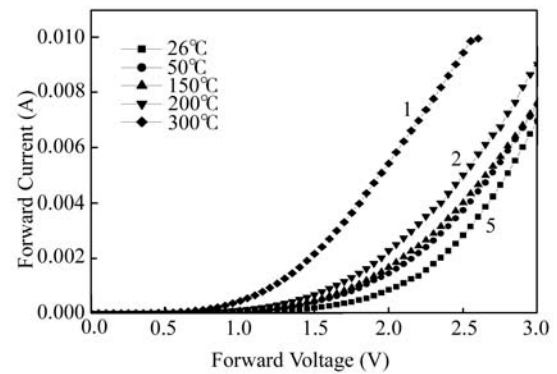


Fig. 5. Forward current-voltage characteristics of  $\text{Au}/\text{Ni}/\text{Al}_x\text{Ga}_{1-x}\text{N}/\text{GaN}$  heterostructure Schottky diodes at various temperatures. Curves 1, 2, 3, 4, and 5 correspond respectively to 300, 200, 150, 50, and 26 °C.

Further, although the charges at the M and S faces of the M/S system increases with increasing (less negative) bias, some of them flow into the 2DEG quantum well. As a result, the slopes of various curves of Fig. 4 do not change much at biases above about  $-1.0$  V. The linearity of the  $C^{-2}$  versus  $V$  plots at various temperatures does not also follow Eq. (1). Nevertheless, the M/S interface characteristics are modified at higher temperatures, which disturb the charge alignment of the M and S faces of the M/S heterostructure.

### 3.2. Current-voltage characteristics

$I$ - $V$  characteristics of the  $\text{Al}_x\text{Ga}_{1-x}\text{N}/\text{GaN}$  Schottky diodes are shown in Fig. 5. Under an applied bias, for example, of 2.5 V, while the current is on the order of  $2.95 \times 10^{-3}$  A at 26 °C, it is on the order of  $9.52 \times 10^{-3}$  A at 300 °C. Thus a significant improvement in the forward conducting current takes place due to increase in thermal biasing. The forward conduction starts at about 0.5 V at 300 °C, but at about 1 V at room temperature. At a certain temperature, the observed variation of current with applied bias is exponential. But at a certain applied bias, the variation of current with temperature is quite slow at  $26$  °C  $\leq T \leq 200$  °C, but quite rapid at  $T > 200$  °C. The trend in the variation of current with applied bias appears to follow the thermionic emission which, for Schottky diodes,

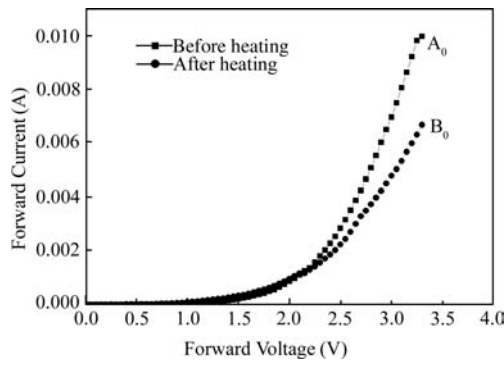


Fig. 6. Forward current–voltage characteristics of  $\text{Al}_x\text{Ga}_{1-x}\text{N}/\text{GaN}$  Schottky diodes before and after heating; curve  $A_0$  was obtained for the diodes before heating, and curve  $B_0$  to was obtained for the diodes after heating, both at room temperature.

is given by<sup>[4]</sup>

$$I = I_0 \exp\left(\frac{qV}{n_{\text{idl}}k_B T}\right) \left[1 - \exp\left(-\frac{qV}{k_B T}\right)\right], \quad (6)$$

where  $I_0$  is the reverse saturation current given by

$$I_0 = AA^*T^2 \exp\left(-\frac{q\phi_B}{k_B T}\right), \quad (7)$$

$A$  is the surface area of the metal–semiconductor interface (area of the diode),  $A^*$  is the Richardson constant,  $V$  is the applied bias,  $\phi_B$  is the Schottky barrier heights, and  $n_{\text{idl}}$  is the ideality factor. However, a close examination of the experimental data suggests that the current is less sensitive to applied bias than it should be under conditions of thermionic emission. The insensitivity stems from an increase in barrier height and an involvement of other mechanisms such as field emission, thermionic field emission, tunneling, generation–recombination, etc.

A comparison of the variation of forward current with applied bias of  $A_0$  and  $B_0$  diodes is shown in Fig. 6.  $A_0$  diodes are the  $\text{Al}_x\text{Ga}_{1-x}\text{N}/\text{GaN}$  diodes kept at room temperature all the time.  $B_0$  diodes are the  $\text{Al}_x\text{Ga}_{1-x}\text{N}/\text{GaN}$  diodes, which underwent a stepwise heating process being kept at each temperature step for about 15 min. More specifically, the device temperature was increased stepwise from room temperature (26 °C) to 50 °C; from 50 to 150 °C; from 150 to 200 °C; and finally from 200 to 300 °C, respectively. The devices were then cooled down back to 26 °C. So, the  $B_0$  diodes underwent some form of thermal annealing. The forward current for both the  $A_0$  and  $B_0$  diodes is obtained at room temperature. Yet these currents are slightly different; the one for the  $B_0$  diodes is lower than the one for the  $A_0$  diodes. This means that the Schottky barrier height for the  $B_0$  diodes is higher than that for the  $A_0$  diodes. The difference between the two may be attributed to the relaxation of strain of the  $\text{Al}_x\text{Ga}_{1-x}\text{N}/\text{GaN}$  heterostructure, formation of alloys, and change in barrier height due to annealing. XRD patterns of Au/Ni/GaN contacts alloyed at various temperatures confirm<sup>[11,12]</sup> that the primary products can be  $\text{Ni}_3\text{N}$  and  $\text{Ni}_4\text{N}$  for an alloying temperature  $0^\circ\text{C} < T_{\text{RTA}} < 200^\circ\text{C}$ . The primary products are  $\text{Ga}_4\text{Ni}_3$ ,  $\text{Ga}_3\text{Ni}_2$ ,  $\text{Ni}_3\text{N}$ ,  $\text{GaAu}$ , and  $\text{GaAu}_2$  for the alloying temperature  $500^\circ\text{C} < T_{\text{RTA}} < 600^\circ\text{C}$ .

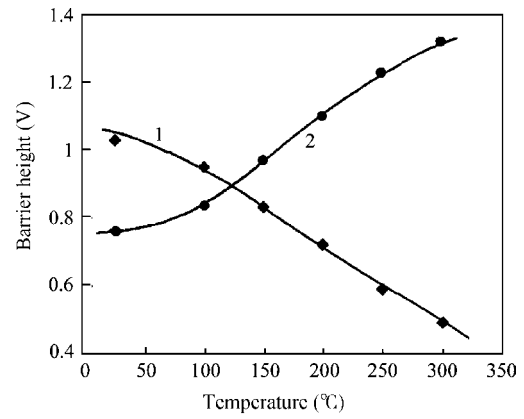


Fig. 7. Temperature dependence of Schottky barrier height of various Schottky barriers. While curve 1 is for  $\text{Al}_x\text{Ga}_{1-x}\text{N}$  diode, curve 2 is for  $\text{Al}_x\text{Ga}_{1-x}\text{N}/\text{GaN}$  diode.

It should also be noted that the 2DEG density dictates the magnitude of the electric field on the GaN side of the  $\text{Al}_x\text{Ga}_{1-x}\text{N}/\text{GaN}$  interface. A higher 2DEG sheet carrier concentration produces a larger electric field in GaN<sup>[13]</sup>. The quantum well channel with a higher electric field at the GaN/ $\text{Al}_x\text{Ga}_{1-x}\text{N}$  interface requires a higher voltage to pinch-off. Because of this, as evidenced from Fig. 5, the current is higher at higher temperature, and lower at lower temperature. The lower current at lower temperature is indicative of the lower 2DEG concentration of the quantum well channel.

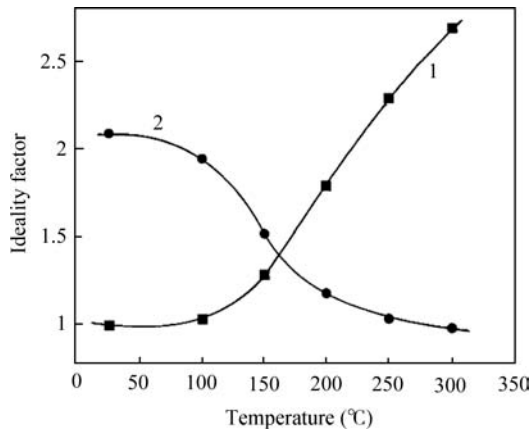
### 3.3. Schottky barrier heights and ideality factor

Figure 7 compares the temperature dependence of the Schottky barrier height  $\phi_B$  of the  $\text{Al}_x\text{Ga}_{1-x}\text{N}$  and  $\text{Al}_x\text{Ga}_{1-x}\text{N}/\text{GaN}$  diodes. The measured variation of barrier height with temperature for the  $\text{Al}_x\text{Ga}_{1-x}\text{N}/\text{GaN}$  Schottky diodes is opposite to that for the  $\text{Al}_x\text{Ga}_{1-x}\text{N}$  Schottky diodes. For the  $\text{Al}_x\text{Ga}_{1-x}\text{N}$  diodes, the barrier height decreases with increasing temperature. At higher temperatures, the thermally activated metal electrons tunnel into the semiconductor depletion region. The M/S depletion width is thus reduced and the Schottky barrier height lowered.

Figure 7 indicates that the barrier heights for the  $\text{Al}_x\text{Ga}_{1-x}\text{N}/\text{GaN}$  diodes, as determined for 26, 100, 150, 200, 250, and 300 °C, are 0.762, 0.835, 0.973, 1.104, 1.233, and 1.321 V, respectively. The barrier height increase is slow at temperatures between 300 and 250 °C, quite rapid at temperatures between 250 and 100 °C, and again quite slow at temperatures between 100 and 26 °C. The  $\text{Al}_x\text{Ga}_{1-x}\text{N}/\text{GaN}$  diodes have quantum well and 2DEG. As a result, some of the thermally activated metal electrons, while tunneling into the semiconductor, are nullified by the polarized induced positive charges; others are transported into quantum wells. More  $\text{Al}_x\text{Ga}_{1-x}\text{N}$  donor atoms are thus ionized at higher temperatures, and the free electrons, thus created, are drifted into the quantum well. The M/S depletion region is consequently widened and the Schottky barrier height enlarged. The change of the barrier heights as a function of temperature for the  $\text{Al}_x\text{Ga}_{1-x}\text{N}$  and  $\text{Al}_x\text{Ga}_{1-x}\text{N}/\text{GaN}$  diodes may empirically be modeled as

Table 1. List of various parameters of the temperature dependent barrier height.

Diode	$\phi_{B0}(0^\circ\text{C})$ , Volt	$\alpha_B$ (V/°C)	$T_B$ (°C)
$\text{Al}_x\text{Ga}_{1-x}\text{N}/\text{GaN}$	0.75	$1.158 \times 10^{-2}$	$1.262 \times 10^3$
$\text{Al}_x\text{Ga}_{1-x}\text{N}$	1.07	$-0.32 \times 10^{-2}$	$1.666 \times 10^2$

Fig. 8. Temperature dependence of ideality factor of various Schottky diodes. While curve 1 is for  $\text{Al}_x\text{Ga}_{1-x}\text{N}$  diode, curve 2 is for  $\text{Al}_x\text{Ga}_{1-x}\text{N}/\text{GaN}$  diode.

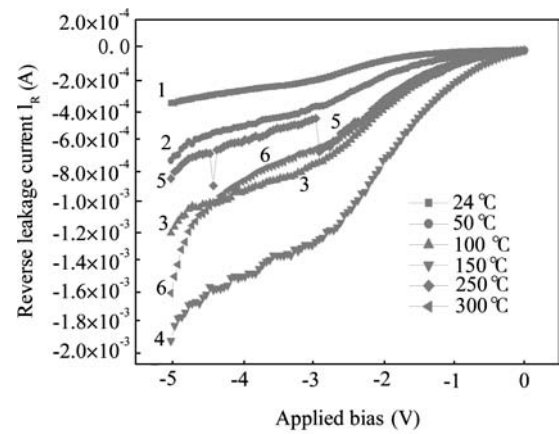
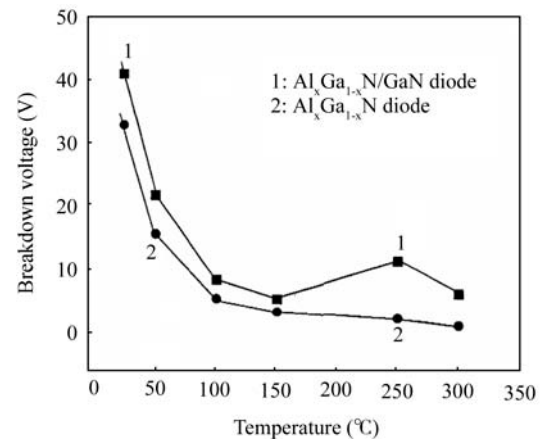
$$\phi_B = \phi_{B0}(0^\circ\text{C}) + \frac{\alpha_B T^2}{T_B + T}, \quad (8)$$

where  $\phi_{B0}(0^\circ\text{C})$ ,  $\alpha_B$ , and  $T_B$  are the various parameters listed in Table 1.

Figure 8 depicts the temperature dependence of the ideality factor. For the  $\text{Al}_x\text{Ga}_{1-x}\text{N}/\text{GaN}$  Schottky diodes, the ideality factor decreases slowly until the temperature is about  $100^\circ\text{C}$ , and then decreases quite rapidly until the temperature reaches about  $250^\circ\text{C}$ . The decrease slows down beyond  $250^\circ\text{C}$ . While the ideality factor is 1.02 at  $300^\circ\text{C}$ , it is 1.198 at  $200^\circ\text{C}$ , and 2.09 at  $26^\circ\text{C}$ . As always, the ideality factor is a measure of the quality of the Schottky diode, and an increase in ideality factor implies that the diode quality decreases at lower temperatures. The situation is reverse for the  $\text{Al}_x\text{Ga}_{1-x}\text{N}$  Schottky diodes, for which the ideality factor is close to unity at room temperature, but quite high at  $300^\circ\text{C}$ . Transport mechanisms such as trap-assisted tunneling, field emission, thermionic field emission, etc. are very highly sensitive to the barrier height. They decrease almost exponentially with increasing barrier height. So, for the  $\text{Al}_x\text{Ga}_{1-x}\text{N}$  Schottky diodes, for which the barrier height decreases with increasing temperature, the forward current is dominated by these transport mechanisms far more at higher temperature than at room temperature. Consequently the ideality factor is larger at higher temperatures. In contrast, for the  $\text{Al}_x\text{Ga}_{1-x}\text{N}/\text{GaN}$  Schottky diodes, for which the barrier height increases with increasing temperature, the forward current at higher temperatures is hardly affected by these transport mechanism.

### 3.4. Reverse leakage and breakdown

The  $\text{Al}_x\text{Ga}_{1-x}\text{N}$  and GaN layer were grown on the lattice mismatched sapphire substrate, and hence exhibit high defect densities such as nanopipes and threading dislocations in the

Fig. 9. Reverse current–voltage characteristics of  $\text{Al}_x\text{Ga}_{1-x}\text{N}/\text{GaN}$  Schottky diodes at various temperatures. Curves 1, 2, 3, 4, 5 and 6 correspond respectively to 24, 50, 100, 150, 250 and  $300^\circ\text{C}$ .Fig. 10. Reverse current–voltage characteristics of  $\text{Al}_x\text{Ga}_{1-x}\text{N}/\text{GaN}$  Schottky diodes at various temperatures. Curves 1, 2, 3, 4, 5 and 6 correspond respectively to 24, 50, 100, 150, 250 and  $300^\circ\text{C}$ .

range of  $(10^8\text{--}10^{10}\text{ cm}^{-2})$  in the material structure. Because of these nanopipes, growth steps and dense pits are inhomogeneously formed on the semiconductor surface. These pits are actually the surface termination of threading dislocations (TDs) exhibiting electronic states near the valence band, which have led to high reverse leakage current and premature breakdown both in the  $\text{Al}_x\text{Ga}_{1-x}\text{N}$  and  $\text{Al}_x\text{Ga}_{1-x}\text{N}/\text{GaN}$  Schottky diodes. For the  $\text{Al}_x\text{Ga}_{1-x}\text{N}$  diodes, the increase in reverse leakage current always accompanies an increase in temperature, which is consistent with the findings of Ip *et al.*<sup>[14]</sup>. For the  $\text{Al}_x\text{Ga}_{1-x}\text{N}/\text{GaN}$  diodes, the reverse leakage current increases first, and then decreases, with increasing temperature (Fig. 9). For these diodes, electrons have higher energy, and Schottky barriers have larger height, at higher temperature. Of these two, higher electron energy promotes leakage, but higher barrier height demotes leakage. Therefore, the reverse leakage current depends on which one of them dominates at which temperature. The trend of this current reflects higher thermal stability of leakage, which results from the piezoelectric polarization of charges and the changes in  $\text{Al}_x\text{Ga}_{1-x}\text{N}$  surface states.

The room temperature breakdown voltages, shown in Fig. 10 for various diodes, indicate improved results for the

$\text{Al}_x\text{Ga}_{1-x}\text{N}/\text{GaN}$  diodes. While, at room temperature, it is about 41 V for the  $\text{Al}_x\text{Ga}_{1-x}\text{N}/\text{GaN}$  diodes, it is about 33 V for the  $\text{Al}_x\text{Ga}_{1-x}\text{N}$  diodes. It deteriorates, however, with increasing temperature. At a temperature of 300 °C, it reduces to about 10 V for the  $\text{Al}_x\text{Ga}_{1-x}\text{N}/\text{GaN}$  diodes, and to about 5 V for the  $\text{Al}_x\text{Ga}_{1-x}\text{N}$  diodes. Thus, hard breakdown room-temperature characteristics do not really exist at high temperatures. The soft breakdown observed at high temperatures is caused mainly by the interface current resulting from the generation of high surface states and/or thermal activation of traps at the M/S interface.

The thermally activated current may result also from the conduction of electrons from metal into the semiconductor(s) along the TDs. An electron in the metal falls into a TD state lying in the vicinity of the Fermi level of the metal, and is subsequently transported away by a one-dimensional variable-range-hopping conduction given by

$$\sigma = \sigma_0 \exp[-(T_0/T)], \quad (9)$$

where  $T_0$  is a characteristic temperature of the electron. The TD density in semiconductor is very high ( $10^9$ – $10^{10} \text{ cm}^{-2}$ ) in the vicinity of sapphire substrate; it is lower, but still significant in the bulk. So, a possible scenario may be that the electrons, which are trapped at deeper levels at room temperature, become more energetic at higher temperatures, and jump up to occupy shallow levels. While the capture and occupancy of electrons (at shallow levels) is mediated by applied electric field at the M/S interface, the emission of these trapped electrons is caused first by activation and then by field-assisted tunneling (see Fig. 2). Obviously, at a certain electric field and temperature, the electron current generated by electron emission from the shallow level traps is much higher than that from the deep level traps. Consequently, the leakage is much lower, and the breakdown voltage is much higher, at lower temperatures than at higher temperatures. While the thermionic emission and field-assisted tunneling are responsible for the emission of trapped electrons at higher temperatures, field-assisted tunneling is crucial for emission at lower temperatures.

In summary, the chemico-physical mechanisms responsible for reverse leakage include thermionic emission over the Schottky barrier, field-emission tunneling, and trap-assisted tunneling through the Schottky barrier. For  $\text{Al}_x\text{Ga}_{1-x}\text{N}$ , the first one may be negligibly small due to large Schottky barrier height. The second one associated with transition from metal into semiconductor is dominant at lower temperatures, and preferably at  $T \leq 300 \text{ K}$ . Our results show that a significant increase in leakage current takes place if the reverse bias exceeds the threshold value, which is about  $-1 \text{ V}$ . This trend occurs because the carrier transport at this reverse bias is dominated by field-emission tunneling and/or trap-assisted tunneling through the Schottky barrier. At  $T \leq 300 \text{ K}$ , the leakage is primarily due to thermal activation of metal electrons to a shallow trap level at the M/S interface, and a subsequent tunneling into the semiconductor. The trap level is related to TDs. Depending on the depth of TD-related trap states, there can be metastable acceptor and/or donor-like states (see

Fig.2) coexisting in the vicinity of TDs and responsible for the local reverse leakage current. Hierro *et al.*<sup>[15]</sup> noted that the TD-related trap states, even with energy levels at 0.91 and 0.59 eV below the conduction band edge, can cause the conduction mechanism of reverse leakage current. However, they both concluded that the trap-assisted tunneling is the dominant conduction mechanism for reverse leakage current. Further, noting that the trap-assisted tunneling is a rate-limiting step, the leakage current is a function of reverse voltage and the inhomogeneity of the spatial distribution of surface pits (e.g., TD terminations). The spatial distribution of surface pits is less inhomogeneous at lower temperatures, and this is why the room-temperature reverse leakage current is almost constant. The shallow level traps created at higher temperature are the probable cause of low breakdown voltages.

## 4. Conclusions

A thorough and in-depth investigation has been carried out to understand the temperature dependent carrier transport and interface properties of the  $\text{Al}_x\text{Ga}_{1-x}\text{N}/\text{GaN}$  Schottky diodes. The characteristics of the  $\text{Al}_x\text{Ga}_{1-x}\text{N}/\text{GaN}$  diodes have been compared with those of the  $\text{Al}_x\text{Ga}_{1-x}\text{N}$  diodes to accomplish the goal. As elucidated earlier, these diodes are extremely important for the realization of modern electronic devices, such as HEMTs. Our investigation strongly demonstrates that the piezoelectric polarization field and 2DEG charge density play crucial roles in dictating the electronic performance of the  $\text{Al}_x\text{Ga}_{1-x}\text{N}/\text{GaN}$  Schottky diodes. Because of the polarization effect, the Schottky barrier height is increased, and the reverse leakage current decreased. Both of them tend to improve the high-temperature performance of HEMTs. Good surface morphology created by appropriate chemical treatment of the surface is crucial for these diodes. Optimal concentration of aqua regia solution and the value of its boiling temperature are the ones that enable such good treatment. So, the identification of a combined aqua regia plus  $\text{NH}_4\text{OH}$  surface treatment for the minimization of surface defect levels and passivation, if not removal, of surface DCBs, is a unique manifestation of the present investigation.

## References

- [1] Mohammad S N, Alvador A, Morkoç H. Emerging gallium nitride based devices. *IEEE Proc*, 1995, 83: 1306
- [2] Aktas O, Kim W, Fan Z, et al. High-transconductance GaN MODFETs. *Technical Digest-International Electron Devices Meeting*, 1995: 205
- [3] Lu C, Chen H, Lv X, et al. Temperature and doping-dependent resistivity of Ti/Au/Pd/Au multilayer ohmic contact to n-GaN. *J Appl Phys*, 2002, 91: 9218
- [4] Motayed A, Sharma A K, Jones K A, et al. Electrical characteristics of  $\text{Al}_x\text{Ga}_{1-x}\text{N}$  Schottky diodes prepared by a two-step surface treatment. *J Appl Phys*, 2004, 96: 3286
- [5] Suzue K, Mohammad S N, Fan Z, et al. Electrical conduction in platinum-gallium nitride Schottky diodes. *J Appl Phys*, 1996, 80: 4467

- [6] Mohammad S N, Fan Z, Botchkarev A E, et al. Near-ideal platinum-GaN Schottky diodes. *Electron Lett*, 1996, 32: 598
- [7] Mohammad S N, Fan Z F, Botchkarev A E, et al. Physical mechanisms underlying anomalous capacitance characteristics of platinum-gallium nitride Schottky diodes. *Philos Mag*, 2001, B81: 453
- [8] Mohammad S N. Contact mechanisms and design principles for alloyed ohmic contacts to n-GaN. *J Appl Phys*, 2004, 95: 7940
- [9] Mohammad S N. Contact mechanisms and design principles for Schottky contacts to group-III nitrides. *J Appl Phys*, 2005, 97: 63703
- [10] Drouin D, Beauvais J, Lemire R, et al. Method for fabricating submicron silicide structures on silicon using a resistless electron beam lithography process. *Appl Phys Lett*, 1997, 70: 3020
- [11] Guo J D, Pan F M, Feng M S, et al. Schottky contact and the thermal stability of Ni on n-type GaN. *J Appl Phys*, 1996, 80: 1623
- [12] Sheu J K, Su Y K, Chi G C, et al. Effect of thermal annealing on the Ni/Au contact of p-type GaN. *J Appl Phys*, 1998, 83: 3172
- [13] Gaska R, Yang J W, Bykhovoski A D, et al. Influence of the deformation on the two-dimensional electron gas density in GaN-AlGaIn heterostructures. *Appl Phys Lett*, 1998, 72: 64
- [14] Ip K, Heo Y W, Baik K H, et al. Temperature-dependent characteristics of Pt Schottky contacts on n-type ZnO. *Appl Phys Lett*, 2004, 84: 2835
- [15] Hierro A, Kwon D, Ringela S A, et al. Optically and thermally detected deep levels in n-type Schottky and p<sup>+</sup>-n GaN diodes. *J Appl Phys*, 2000, 76: 3064